

# Soft-output (SO) GRAND and Iterative Decoding to Outperform LDPCs

Peihong Yuan, *Member, IEEE*, Muriel Médard, *Fellow, IEEE*, Kevin Galligan, and Ken R. Duffy, *Senior Member, IEEE*

**Abstract**—We establish that a large, flexible class of long, high redundancy error correcting codes can be efficiently and accurately decoded with guessing random additive noise decoding (GRAND). Performance evaluation demonstrates that it is possible to construct simple product codes with lengths of approximately 200 to 4000 bits and rates between 0.2 and 0.8 that outperform low-density parity-check (LDPC) codes from the 5G New Radio standard in both AWGN and fading channels. The concatenated structure enables many desirable features, including: low-complexity hardware-friendly encoding and decoding; significant flexibility in length and rate through modularity; and high levels of parallelism in encoding and decoding that enable low latency.

Central is the development of a method through which any soft-input (SI) GRAND algorithm can provide soft-output (SO) in the form of an accurate a-posteriori estimate of the likelihood that a decoding is correct or, in the case of list decoding, the likelihood that each element of the list is correct. The distinguishing feature of soft-output GRAND (SOGRAND) is the provision of an estimate that the correct decoding has not been found, even when providing a single decoding. That per-block SO can be converted into accurate per-bit SO by a weighted sum that includes a term for the SI. Implementing SOGRAND adds negligible computation and memory to the existing decoding process, and using it results in a practical, low-latency alternative to LDPC codes.

**Index Terms**—GRAND, concatenated codes, product codes, LDPC, Generalized LDPC

## I. INTRODUCTION

Since Shannon’s pioneering work [2], the quest to design efficiently decodable long, high-redundancy error correction codes has resulted in technical revolutions from product codes [3] to concatenated codes [4] to turbo codes [5] to turbo product codes [6] to low-density parity-check (LDPC) codes [7, 8]. Since the rediscovery of LDPC codes in the 1990s [9–11] and the subsequent development of practical encoders and decoders, e.g. [12–18], they have become the gold standard for high performance, long, large redundancy, SI error correction codes. They are used, for example, in standards including ATSC 3.0 [19] and 5G New Radio [20].

This paper was presented in part at 2023 IEEE Globecom [1].

P. Yuan and M. Médard are with the Massachusetts Institute of Technology Network Coding & Reliable Communications Group (e-mails: {phyuan, medard}@mit.edu).

K. Galligan is with the Maynooth University Hamilton Institute, (e-mail: kevin.galligan.2020@mumail.ie).

K. R. Duffy is with the Northeastern University Engineering Probability Information & Communications Laboratory (e-mail: k.duffy@northeastern.edu).

This work was supported by the Defense Advanced Research Projects Agency (DARPA) under Grant HR00112120008. (*Corresponding author: Muriel Médard*)

A common principle behind the design of long, high-redundancy codes is to create them by concatenating and composing shorter component codes. With soft-input (SI), each component is decoded and provides soft-output (SO) that informs the decoding of another component. The process is repeated, passing updated soft information around the code until a global consensus is found or the effort is abandoned. Core to performance is a combination of code-structure, which determines how soft information is circulated amongst components, and the quality of the decoder’s SO, which captures how much is gleaned from each decoding of a component code. E.g., turbo decoding of Elias’s product codes [3] can avail of powerful component codes, such as Bose-Chaudhuri-Hocquenghem (BCH) codes, but relies on approximate SO [6], while LDPC codes avail of weak single parity-check codes but provide high quality per-component SO.

Guessing random additive noise decoding (GRAND) is a recently developed family of code-agnostic decoding algorithms that can accurately decode any moderate redundancy code in both hard [21–23] and soft detection [24–28] settings. GRAND algorithms function by sequentially inverting putative noise effects, ordered from most to least likely according to channel properties and soft information, from received signals. The first codeword yielded by inversion of a noise effect is a maximum-likelihood decoding. Since this procedure does not depend on codebook structure, GRAND can decode any moderate redundancy code, even non-linear ones [29]. Efficient hardware implementations [30–32] and syntheses [33–36] for both hard and soft-detection settings have established the flexibility and energy efficiency of GRAND decoding strategies.

Here we significantly extend GRAND’s range of operation by developing SO variants that can be used to accurately and efficiently decode long, high-redundancy codes. While initial attempts have used GRAND solely as a list decoder [37–39] with Pyndiah’s traditional approach to generate SO [6], central to the enhanced performance here is proving that any SI GRAND algorithm can itself readily produce more accurate SO. This enhancement results in better block error rate (BLER) and bit error rate (BER) performance as well as lower complexity.

The SO measure we develop is an accurate estimate of the a-posteriori probability (APP) that a decoding is correct in the case of a single decoding, and, in the case of list decoding, the probability that each codeword in the list is correct or the correct codeword is not in the list. We derive these probabilities for uniform at random codebooks and demonstrate that the resulting formulae continue to provide

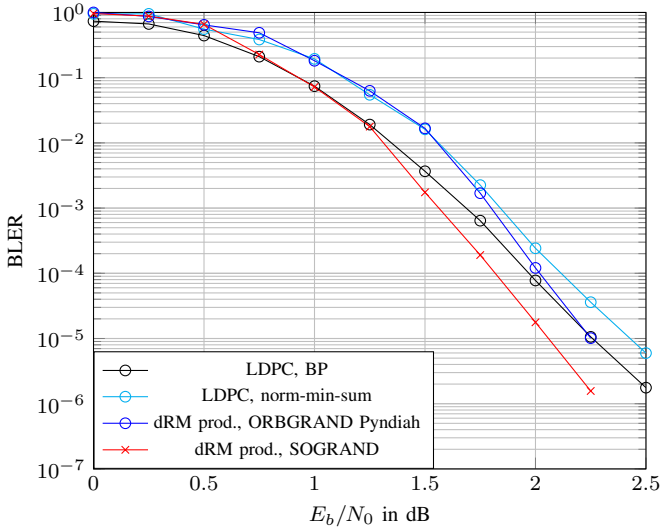


Fig. 1: additive white Gaussian noise (AWGN) BLER performance of the (1024, 441) 5G LDPC with maximum iteration number 50 as compared to a (1024, 441) = (32, 21)<sup>2</sup> dRM product code decoded two ways. First, turbo-decoded [6], with  $\alpha$  and  $\beta$  parameters taken from there and maximum iteration number 20, but using 1line-ORBGRAND for list decoding with list size  $L = 4$  as in [38]. Second, turbo-decoded using  $\alpha = 0.5$  and SOGRAND with max iteration 20, where lists are added to until  $L = 4$  or the predicted list-BLER is below  $10^{-5}$ .

accurate SO for structured codebooks. The formulae can be used with any algorithm in the GRAND family regardless of the algorithm’s query order.

Calculating the SO only requires knowledge of the code’s dimensions and the evaluation of the probability of each noise effect query during GRAND’s normal operation, so computation of the measure does not significantly increase the decoder’s algorithmic complexity or memory requirements.

In Forney’s seminal work [40], the classical per-block SO approximation from list decoding is the conditional probability that an element of the list is the decoding given the transmitted codeword is in the list. The core distinction of soft-output GRAND (SOGRAND) is that it foregoes the conditioning by inherently including an estimate of the likelihood that the correct decoding has not been found. Its use significantly improves the quality of the information that circulates after decoding a component code and, in contrast to LDPC codes, allows the practical use of powerful component codes with multiple bits of redundancy.

The merit of SOGRAND is demonstrated in Fig. 1 where BLER vs  $E_b/N_0$  in dB for the (1024, 441) LDPC in the 5G New Radio standard decoded with belief propagation (BP) or min-sum [41] is plotted in the standard AWGN setting. Also shown is the performance of a simple product code [3], a (1024, 441) = (32, 21)<sup>2</sup> dynamic Reed Muller (dRM) code [42], decoded two distinct ways. Using Pyndiah’s original SO methodology [6, 38] but with a list provided by the 1-line version of ordered reliability bits GRAND (ORBGRAND)

[25] that enhances its performance over traditional Chase decoding, the product code mildly under-performs in comparison to the LDPC code. Decoding with the new SOGRAND algorithm developed here sees the product code get a ca. 0.2 dB gain in performance and outperforming the LDPC code. It will be shown in Sec. VI that this improved performance comes with reduced complexity, consistent with previous findings for GRAND algorithms, and that the gain is sustained in channels subject to fading.

Comparison of LDPC codes and product codes of other dimensions are shown in Sec. VI and establish consistent or better findings: when decoded with SOGRAND, Elias’s product codes provide better performance than state-of-the-art codes and do so with modest complexity and minimal latency. Variants on the theme of product codes, such as staircase codes [43] and generalized low-density parity-check (GLDPC) codes [44], were developed to enhance the minimum distance of the original design. In section VI we show that decoding the GLDPC code proposed in [45] with SOGRAND results in significantly steeper BLER curves and better performance than LDPC codes in the 5G standard at higher SNR.

## II. PER-BLOCK SO

For any channel coding scheme it would be desirable if error correction decoders could produce SO in the form of a confidence measure in the correctness of a decoded block. In seminal work on error exponents, Forney [40] proposed an approximate computation that necessitates the use of a list decoder. It takes the form of a conditional likelihood of correctness given the codeword is in the list. We shall demonstrate that the approach provides an inaccurate estimate in channels with challenging noise conditions. Regardless, its potential utility motivated further investigation, e.g. [46].

With the recent introduction of CRC-assisted successive cancellation list (CA-Polar) codes to communications standards [47], Forney’s approximation has received renewed interest [48] as one popular method of decoding CA-Polar codes, CRC-assisted successive cancellation list (CA-SCL) decoding, generates a list of candidate codewords as part of its execution, e.g. [49–51]. For convolution or trellis codes, the Viterbi algorithm [52] can be modified to produce SO at the sequence level [53], which has been used in coding schemes with multiple layers of decoding [54] and to inform repeat transmission requests [55][53].

SOGRAND can be used with any moderate redundancy component code, which opens up a large palette of possibilities. Unlike Forney-style approaches, it includes a term for the likelihood that the correct decoding has not yet been found. As a result, it can be evaluated without the need to list decode and the estimate remains accurate in noisy channel conditions. From it, accurate per-bit SO can be created through a weighted mixture of identified decodings and SI with the likelihood that the decoding is not an element of the list.

## III. PRELIMINARIES

### A. Notations

Let  $\mathcal{C}$  be a codebook containing  $2^k$  binary codewords each of length  $n$  bits. Let  $X^n$  be a codeword drawn uniformly at

random from the codebook and let  $N^n$  denote the binary noise effect that the channel has on that codeword during transmission; that is,  $N^n$  encodes the binary difference between the demodulated received sequence and the transmitted codeword. Then  $Y^n = X^n \oplus N^n$  is the demodulated channel output, with  $\oplus$  being the element-wise binary addition operator. Let  $R^n$  denote real soft channel output per-bit. Lowercase letters represent realizations of random variables (RVs), with the exception of  $z^n$ , which is the realization of  $N^n$ , which is assumed independent of the channel input. We denote the memoryless channel by  $f_{R|X}$  and represent both the probability density function (PDF) and probability mass function (PMF) of the RV  $X$  as  $p_X(x)$ .

### B. Background on GRAND

All GRAND algorithms operate by progressing through a series of noise effect guesses  $z^{n,1}, z^{n,2}, \dots \in \{0, 1\}^n$ , whose order is informed by channel statistics, e.g. [23], or SI, e.g. [25], until it finds one,  $z^{n,q}$ , that satisfies  $\hat{x}_q^n = y^n \ominus z^{n,q} \in \mathcal{C}$ , where  $\ominus$  inverts the effect of the noise on the channel output. If the guesses are in decreasing order of likelihood, then  $z^{n,q}$  is a maximum-likelihood estimate of  $N^n$  and  $\hat{x}_q^n$  is a maximum-likelihood estimate of the transmitted codeword  $X^n$ . Since this guessing procedure does not depend on codebook structure, GRAND can decode any moderate redundancy code as long as it has a method for checking codebook membership. For a linear block code with an  $(n-k) \times n$  parity-check matrix  $\mathbf{H}$ ,  $\hat{x}_q^n$  is a codeword if  $\mathbf{H}\hat{x}_q^n = 0^n$  [56], where  $\hat{x}_q^n$  is taken to be a column vector and  $0^n$  is the zero vector. To generate a decoding list  $\mathcal{L}$  of size  $L$ , GRAND's guessing procedure continues until  $L$  codewords are found [26, 38].

While GRAND algorithms can decode any block code, so-called "even" linear block codes, e.g. [56], offer a complexity advantage at no cost in decoding performance so long as the GRAND query generator can skip patterns of a certain Hamming weight [57]. A binary linear code with generator matrix  $\mathbf{G} = \{\mathbf{G}_{i,j}\}$  is even if, with addition in  $\mathbb{F}_2$ ,  $\sum_{j=1}^n \mathbf{G}_{i,j} = 0$  for all  $i \in \{1, \dots, k\}$  as that ensures that  $\sum_{i=1}^n c_i = 0$  for every  $c^n \in \mathcal{C}$ . Consequently, if a codeword,  $c^n$ , is perturbed by a channel,  $y^n = c^n + z^n$ , then

$$\sum_{i=1}^n y_i = \sum_{i=1}^n (c_i + z_i) = \sum_{i=1}^n c_i + \sum_{i=1}^n z_i = \sum_{i=1}^n z_i$$

and the parity of the demodulated bits  $y^n$  matches the parity of the noise-effect  $z^n$  that has impacted the codeword  $c^n$ .

Thus, if an even code is decoded with a GRAND algorithm that has a mechanism to generate noise-effect sequences of given Hamming weight, only noise effect sequences whose parity is the same as  $\sum_{i=1}^n y_i$  need be generated. The use of this property can reduce the total query number by a factor of up to 2, but the performance is the same as if sequences of any Hamming weight were generated as sequences of mismatched Hamming weight cannot lead to the identification of a codebook element. For soft detection ORBGRAND algorithms implemented with the landslide algorithm [25, 31], it is trivial to skip given Hamming weights and so this approach

is employed here whenever even codes are used. Note that ORBGRAND has been proven to approach capacity [58].

Many codes are inherently even, including extended Bose-Chaudhuri-Hocquenghem (eBCH) codes, polar codes [59] and dRM codes [42] codes. In general, given a generator,  $\mathbf{G}$ , for a code that is not even, it is straight-forward to extend it by setting  $\mathbf{G}_{i,n+1} = \sum_{j=1}^n \mathbf{G}_{i,j}$  in  $\mathbb{F}_2$  for each  $i \in \{1, \dots, k\}$ , which adds one bit to the code and results in an even code.

Underlying GRAND is a race between two RVs, the number of guesses until the true codeword is identified and the number of guesses until an incorrect codeword is identified. Whichever of these processes finishes first determines whether the decoding identified by GRAND is correct. In the SI setting, the guesswork function  $G : \{0, 1\}^n \rightarrow \{1, \dots, 2^n\}$  depends on SI,  $R^n$ , and maps a noise effect sequence to its position in GRAND's guessing order, so that  $G(z^{n,i}) = i$ . Thus  $G(N^n)$  is a RV that encodes the number of guesses until the transmitted codeword would be identified. As  $N^n$  is independent of  $X^n$ , we have that

$$P(G(N^n) = q | R^n = r^n) = p_{N^n | R^n}(z^{n,q} | r^n).$$

Consequently, as  $Y^n = X^n \oplus N^n$ , for any  $c^n \in \mathcal{C}$

$$p_{X^n | R^n}(c^n | r^n) = P(N^n = c^n \oplus y^n | R^n = r^n, N^n \oplus y^n \in \mathcal{C})$$

If  $U_{(i)} : \Omega \rightarrow \{1, \dots, 2^n - 1\}$  is the number of guesses until the  $i$ -th incorrect codeword would be identified, not accounting for the query that identifies the correct codeword, then GRAND returns a correct decoding whenever  $G(N^n) \leq U_{(1)}$  and a list of length  $L$  containing the correct codeword whenever  $G(N^n) \leq U_{(L)}$ . Stochastic analysis of the race between these two processes leads to the derivation of the SO in this paper.

### C. Background on SO

Given channel output  $r^n$ , which serves as SI to the decoder, and a decoding output  $c^{n,*} \in \mathcal{C}$ , the probability that the decoding is correct is

$$p_{X^n | R^n}(c^{n,*} | r^n) = \frac{f_{R^n | X^n}(r^n | c^{n,*})}{\sum_{c^n \in \mathcal{C}} f_{R^n | X^n}(r^n | c^n)}. \quad (1)$$

Based on this formula, in Forney's work on error exponents [40] he derived an optimal threshold for determining whether a decoding should be marked as an erasure. Evaluating the sum in the denominator requires  $2^k$  computations, which is infeasible for codebooks of practical size. Thus, given a decoding list  $\mathcal{L} \subseteq \mathcal{C}$  with  $L \geq 2$  codewords, Forney suggested the approximation

$$p_{X^n | R^n}(c^{n,*} | r^n) \approx \frac{f_{R^n | X^n}(r^n | c^{n,*})}{\underbrace{\sum_{c^n \in \mathcal{L}} f_{R^n | X^n}(r^n | c^n) + \sum_{c^n \in \mathcal{C} \setminus \mathcal{L}} f_{R^n | X^n}(r^n | c^n)}_{\text{assumed to be 0}}}, \quad (2)$$

which is the conditional probability that each element of the list is correct given that the transmitted codeword is in the list. With  $c^{n,*} = \arg \max_{c^n \in \mathcal{L}} f_{R^n | X^n}(r^n | c^n)$ , Forney's approximation results in an estimate of the correctness probability of

$c^{n,*}$  that is no smaller than  $1/L$ . Having the codewords of highest likelihood in the decoding list gives the most accurate approximation as their likelihoods dominate the sum.

A significant source of improvement in the SO that results from the method developed here for GRAND is that it provides an accurate, non-zero estimate of final term in the denominator of eq. (2), even with a single decoding, i.e.  $L = 1$ . As a result, it generates an estimate that is not conditioned on the codeword having been found. That enables an estimate of the likelihood of correctness of a single decoding, i.e. for  $L = 1$ , which is not possible from Forney's approximation, as well as an estimate of the likelihood that the decoding has not been found (i.e. is not in the list):

$$p_{X^n|R^n}(\mathcal{C}\setminus\mathcal{L}|r^n) = \frac{\sum_{c^n \in \mathcal{C}\setminus\mathcal{L}} f_{R^n|X^n}(r^n|c^n)}{\sum_{c^n \in \mathcal{C}} f_{R^n|X^n}(r^n|c^n)}. \quad (3)$$

It is this distinctive feature that enables enable substantially improved SO.

One downside of Forney's approach is that it requires a list of codewords, which most decoders do not provide. For this reason, a method has recently been proposed to estimate the likelihood of the second-most likely codeword given the first [60]. A variety of schemes have also been suggested for making erasure decisions, e. [61].

#### IV. GRAND PER BLOCK SO

Throughout this section, we shall assume that the codebook,  $\mathcal{C}$ , consists of  $2^k$  codewords drawn uniformly at random from  $\{0, 1\}^n$ , although the derivation generalises to higher-order symbols. We first derive exact expressions, followed by readily computable approximations, for the probability that the transmitted codeword is each element of a decoding list or is not contained within it. As a corollary, we obtain a formula for the probability that a single-codeword GRAND output is incorrect. In Section V we demonstrate the formulae provide excellent estimates for structured codebooks.

**Theorem 1** (GRAND list decoding APPs for a uniformly random codebook). *Given the soft information  $R^n = r^n$  that determines the query order, let  $G(N^n)$  be the number of codebook queries until the noise effect sequence  $N^n$  is identified. Let  $W_1, \dots, W_{2^k-1}$  be selected uniformly at random without replacement from  $\{1, \dots, 2^n - 1\}$  and define their rank-ordered version  $U_{(1)} < \dots < U_{(2^k-1)}$ . With the true noise effect not counted,  $U_{(i)}$  corresponds to the location in the guesswork order of the  $i$ -th erroneous decoding in a codebook constructed uniformly-at-random. Define the partial vectors  $U_{(i)}^j = (U_{(i)}, \dots, U_{(j)})$  for each  $i \leq j \in \{1, \dots, 2^k - 1\}$ .*

*Assume that a list of  $L \geq 1$  codewords are identified by a GRAND decoder at query numbers  $q_1 < \dots < q_L$ .<sup>1</sup> Define the associated partial vectors  $q_i^j = (q_i, \dots, q_j)$  for each  $i \leq j \in \{1, \dots, 2^k - 1\}$ , and*

$$q_1^{L,\{i\}} = (q_1, \dots, q_{i-1}, q_{i+1} - 1, \dots, q_L - 1), \quad (4)$$

<sup>1</sup> $q_i$  denotes the query number of the  $i$ -th found codeword. Note that the  $i$ -th found codeword is not necessarily the  $i$ -th most likely codeword.

*which is the vector  $q_1^L$  but with the entry  $q_i$  omitted and one subtracted for all entries from  $q_{i+1}$  onwards. Define*

$$P(A) = \sum_{q > q_L} p_{N^n|R^n}(z^{n,q}|r^n) p_{U_{(1)}^L}(q_1^L)$$

*which is associated with the transmitted codeword not being in the list, and, for each  $i \in \{1, \dots, L - 1\}$ ,*

$$P(B_i) = p_{N^n|R^n}(z^{n,q_i}|r^n) p_{U_{(1)}^{L-1}}(q_1^{L,\{i\}}),$$

*which is associated with the transmitted codeword being the  $i$ -th element of the list, and*

$$P(B_L) = p_{N^n|R^n}(z^{n,q_L}|r^n) \sum_{q \geq q_L} p_{U_{(1)}^{L-1}, U_{(L)}}(q_1^{L-1}, q),$$

*which is associated with the transmitted codeword being the final element of the list. Then the probability that  $i$ -th codeword is correct is*

$$p_{X^n|R^n}(y^n \oplus z^{n,q_i}|r^n) = \frac{P(B_i)}{\sum_{i=1}^L P(B_i) + P(A)} \quad (5)$$

*and the probability that the correct decoding is not in the list is*

$$p_{X^n|R^n}(\mathcal{C}\setminus\mathcal{L}|r^n) = \frac{P(A)}{\sum_{i=1}^L P(B_i) + P(A)}. \quad (6)$$

*Proof.* For  $q \in \{1, \dots, 2^n\}$ , define  $U_{(i),q} = U_{(i)} + 1_{\{U_{(i)} \geq q\}}$ , so that any  $U_{(i)}$  that is greater than or equal to  $q$  is incremented by one. Note that  $U_{(i),G(N^n)}$  encodes the locations of erroneous codewords in the guesswork order of a randomly constructed codebook given the value of  $G(N^n)$  and, in particular,  $U_{(i),G(N^n)}$  corresponds the number of queries until the  $i$ -th incorrect codeword is found given  $G(N^n)$ .

Given the soft information  $R^n = r^n$  that determines the query order, we identify the event that the decoding is not in the list as

$$A = \left\{ G(N^n) > q_L, U_{(1)}^L = q_1^L \right\}$$

and the events where the decoding is the  $i$ -th element of the list by

$$B_i = \left\{ U_{(1)}^{i-1} = q_1^{i-1}, G(N^n) = q_i, \right. \\ \left. U_{(i)}^{L-1} + 1 = q_{i+1}^L, U_{(L)} \geq q_L \right\}$$

where the final condition is automatically met for  $i = \{1, \dots, L - 1\}$  but not for  $i = L$ . The conditional probability that a GRAND decoding is not one of the elements in the list given that  $L$  elements have been found is

$$P\left(A \middle| A \bigcup_{i=1}^L B_i, R^n = r^n\right) \\ = P(A|R^n = r^n) / P\left(A \bigcup_{i=1}^L B_i \middle| R^n = r^n\right). \quad (7)$$

As the  $A$  and  $B_i$  events are disjoint, to compute eq. (7) it suffices to simplify  $P(A)$  and  $P(B_i)$  for  $i \in \{1, \dots, L\}$  to evaluate the APPs.

Consider the numerator,

$$\begin{aligned} P(A) &= P(G(N^n) > q_L, U_{(1)}^L = q_1^L | R^n = r^n) \\ &= \sum_{q > q_L} p_{N^n | R^n}(z^{n,q} | r^n) p_{U_{(1)}^L}(q_1^L), \end{aligned}$$

where we have used the fact that  $G(N^n)$  is independent of  $U_{(1)}^L$  by construction. In considering the denominator, we need only be concerned with the terms  $P(B_i)$  corresponding to a correct codebook being identified at query  $q_i$ , for which

$$\begin{aligned} P(B_i) &= P(G(N^n) = q_i, U_{(1)}^{i-1} = q_1^{i-1}, \\ &\quad U_{(i)}^{L-1} + 1 = q_{i+1}^L, U_{(L)} \geq q_L | R^n = r^n) \\ &= P(G(N^n) = q_i, U_{(1)}^{L-1} = q_1^{L,\{i\}}, U_{(L)} \geq q_L | R^n = r^n) \\ &= p_{N^n | R^n}(z^{n,q_i} | r^n) \sum_{q \geq q_L} p_{U_{(1)}^{L-1}, U_{(L)}}(q_1^{L,\{i\}}, q), \end{aligned}$$

where we have used the definition of  $q_1^{L,\{i\}}$  in eq. (4) and independence. Thus the conditional probability that the correct answer is not found in eq. (7) is given in eq. (6) and the conditional probability that a given element of the list is correct is given by eq. (5).  $\square$

As a result of Theorem 1, to compute the list decoding APPs one needs to evaluate or approximate:

- 1)  $p_{N^n | R^n}(z^{n,q} | r^n)$  and  $\sum_{j \leq q} p_{N^n | R^n}(z^{n,j} | r^n)$ ;
- 2)  $p_{U_{(1)}^L}(q_1^L)$  and  $\sum_{q \geq q_L} p_{U_{(1)}^{L-1}, U_{(L)}}(q_1^{L-1}, q)$ .

During a GRAND algorithm's execution, the evaluation of 1) can be achieved by calculating the likelihood of each noise effect query as it is made and retaining a running sum. For 2), geometric approximations, whose asymptotic precision can be verified using the approach described in [21, Theorem 2], can be employed, result in the following corollaries for list decoding and single-codeword decoding, respectively. Note that these estimates only need to know the code dimensions,  $n$  and  $k$ , rather than any specifics of the code construction.

**Corollary 1** (Approximate APPs for a random codebook). *If each  $U_{(i)}$  given  $U_{(i-1)}$  is assumed to be geometrically distributed with probability of success  $(2^k - 1)/(2^n - 1)$ , then eq. (5) describing the APP that  $i$ -th found decoding is correct,  $p_{X^n | R^n}(y^n \oplus z^{n,q_i} | r^n)$  can be approximated as*

$$\frac{p_{N^n | R^n}(z^{n,q_i} | r^n)}{\sum_{i=1}^L p_{N^n | R^n}(z^{n,q_i} | r^n)} + \left(1 - \sum_{j=1}^{q_L} p_{N^n | R^n}(z^{n,j} | r^n)\right) \left(\frac{2^k - 1}{2^n - 1}\right) \quad (8)$$

and the probability that the list does not contain the transmitted codeword,  $p_{X^n | R^n}(\mathcal{C} \setminus \mathcal{L} | r^n)$  approximated by

$$\frac{\left(1 - \sum_{j=1}^{q_L} p_{N^n | R^n}(z^{n,j} | r^n)\right) \left(\frac{2^k - 1}{2^n - 1}\right)}{\sum_{i=1}^L p_{N^n | R^n}(z^{n,q_i} | r^n)} + \left(1 - \sum_{j=1}^{q_L} p_{N^n | R^n}(z^{n,j} | r^n)\right) \left(\frac{2^k - 1}{2^n - 1}\right) \quad (9)$$

*Proof.* Define the geometric distribution's probability of success to be  $\phi = (2^k - 1)/(2^n - 1)$ . Under the assumptions of the corollary, we have the formulae

$$p_{U_{(1)}^L}(q_1^L) = (1 - \phi)^{q_L - L} \phi^L,$$

for  $i \in \{1, \dots, L - 1\}$

$$p_{U_{(1)}^{L-1}}(q_1^{L,\{i\}}) = (1 - \phi)^{q_L - L} \phi^{L-1},$$

and

$$P\left(U_{(1)}^{L-1} = q_1^{L-1}, U_{(L)} \geq q_L\right) = (1 - \phi)^{q_L - L} \phi^{L-1}.$$

Using those expressions, simplifying eq. (5) gives eq. (8) and eq. (6) gives eq. (9).  $\square$

Taken together, this theorem and corollary provide a simple methodology by which GRAND can provide an APP of the correctness of each element of a decoding list, as well as the likelihood that the correct decoding has not been found.

The proposed SOGRAND algorithm is compatible with any GRAND algorithm. In addition to the usual operations required for GRAND, we require the following additional computations: during the initialization phase, the probability of all-zero noise, i.e.,  $p_{N^n | R^n}(0^n | r^n)$ , is computed. Each time GRAND generates a test pattern  $z^n$ , we need to compute the probability of this pattern  $p_{N^n | R^n}(z^n | r^n)$  and accumulate it accordingly. The term  $p_{N^n | R^n}(z^n | r^n)$  can be computed based on  $p_{N^n | R^n}(0^n | r^n)$ , which needs  $w(z^n)$  operations, where  $w(z^n)$  denotes the Hamming weight of the test noise pattern  $z^n$ , which is usually sparse. In total, we need  $q + \sum_{j=1}^q w(z^{n,j})$  additional operations and store additional values, such as the probability of all-zero noise, the probability of the current guess and the accumulation of these guesses.

## V. SO ACCURACY

### A. Blockwise SO accuracy

Armed with the approximate APP formulae, we investigate its precision for random and structured codebooks. Transmissions were simulated using an AWGN channel with binary phase-shift keying (BPSK) modulation. ORBGRAND [25] was used for SI decoding, which produced decoding lists of the appropriate size for both SO methods. Fig. 2 plots the empirical list-BLER given the predicted list-BLER evaluated using eq. (9). A list error occurs when the transmitted codeword is not in the list of size  $L$ . If the estimate was precise, then the plot would follow the line  $x = y$ , as the predicted

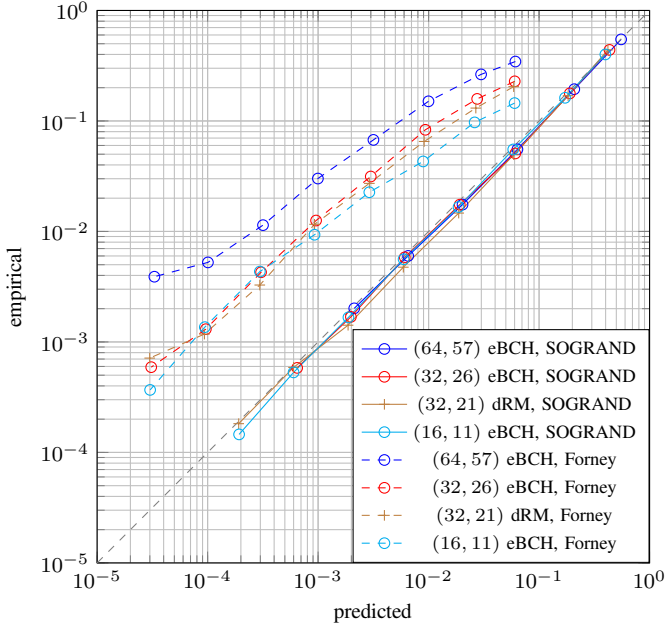


Fig. 2: Predicted list-BLER based on soft-output vs. empirical list-BLER ( $L' = 4$ ): SOGRAND with  $L = 4$ , Forney with  $L = 5$ ,  $E_b/N_0 = 2$ .

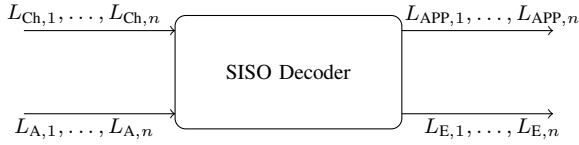


Fig. 3: Soft-Input Soft-Output (SISO) decoder schematic.

list-BLER and the list-BLER would match. It can be seen that SOGRAND provides near perfect estimates for codes of different structures and dimensions.

### B. Bitwise SO accuracy

For many applications, the system requires post-decoding bitwise SO. Fig. 3 shows the inputs and outputs of a soft-input soft-output (SISO) decoder. A SISO decoder takes the sum of channel log-likelihood ratios (LLRs)  $L_{Ch,i}$  and a-priori LLRs  $L_{A,i}$  as input, where

$$L_{Ch,i} = \log \frac{p_{R|X}(r_i|0)}{p_{R|X}(r_i|1)}, \quad L_{A,i} = \log \frac{p_{X_i}(0)}{p_{X_i}(1)}, \quad i = 1, \dots, n.$$

and returns APP LLRs  $L_{APP,i}$  and extrinsic LLRs  $L_{E,i}$  as output, where

$$L_{APP,i} = \log \frac{p_{X_i|R^n}(0|r^n)}{p_{X_i|R^n}(1|r^n)}, \quad L_{E,i} = L_{APP,i} - L_{A,i} - L_{Ch,i},$$

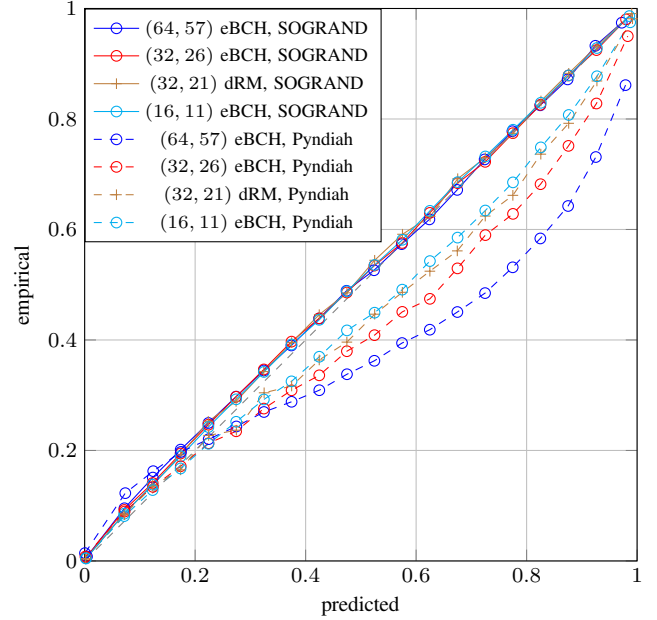


Fig. 4: SO predicted vs. empirical BER:  $L = 4$ ,  $E_b/N_0 = 2$ .

for  $i \in \{1, \dots, n\}$ . Based on the APPs approximations in eq. (8) and (9), the bitwise SO APP LLRs  $L_{APP,i}$  is

$$L'_{APP,i} = \log \frac{\sum_{c^n \in \mathcal{L}: c_i=0} p_{X^n|R^n}(c^n|r^n) + p_{X^n|R^n}(C \setminus \mathcal{L}|r^n) p_{X|R_i}(0|r_i)}{\sum_{c^n \in \mathcal{L}: c_i=1} p_{X^n|R^n}(c^n|r^n) + p_{X^n|R^n}(C \setminus \mathcal{L}|r^n) p_{X|R_i}(1|r_i)} \quad (10)$$

which reflects the content of each codeword in the list and its likelihood, in addition to the likelihood that the codeword is not found whereupon the prior information is retained.

When compared to Pyndiah's approximation,

$$\log \frac{\max_{c^n \in \mathcal{L}: c_i=0} p_{X^n|R^n}(c^n|r^n)}{\max_{c^n \in \mathcal{L}: c_i=1} p_{X^n|R^n}(c^n|r^n)}$$

eq. (9) introduces an additional term that dynamically adjusts the weight between the decoding observations and channel observation. Furthermore, eq. (9) eliminates the need for the saturation value present in Pyndiah's approximation. Fig. 4 shows the BER prediction obtained from eq. (10) and ORBGRAND decoding. The simulated results show that the new SOGRAND approach predicts the BER accurately across a range of channel conditions, code rates and types.

## VI. LONG CODE PERFORMANCE EVALUATION

For iterative decoding, we construct two types of long codes based on short  $(n, k)$  component codes:  $(n^2, k^2)$  product codes [3] and  $(n^2, n^2 - 2n(n - k))$  quasi-cyclic (QC)-GLDPCs [45] with adjacency matrix

$$\begin{bmatrix} I_n^{(0)} & I_n^{(0)} & \dots & I_n^{(0)} \\ I_n^{(0)} & I_n^{(1)} & \dots & I_n^{(n-1)} \end{bmatrix},$$

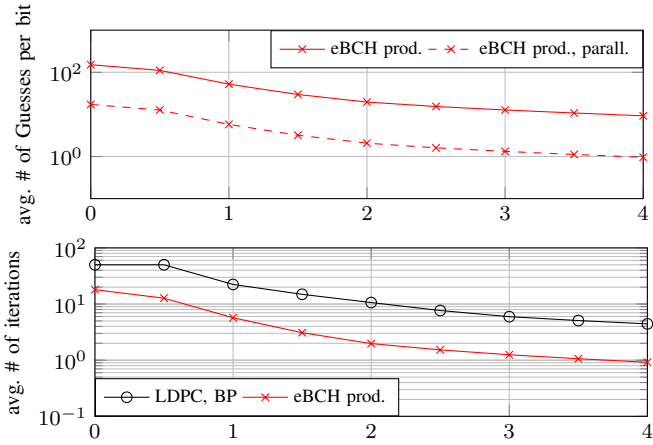
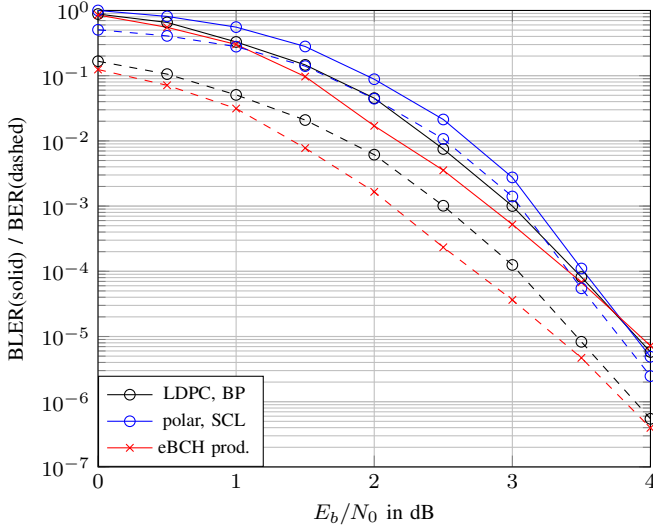


Fig. 5: AWGN performance of  $(256, 121)$  5G LDPC with max. iterations 50 and the  $(256, 121)$  5G CA-Polar (24-bits CRC) decoded with CA-SCL ( $L = 16$ ) as compared to a  $(256, 121) = (16, 11)^2$  eBCH product code decoded with SOGRAND, with  $\alpha = 0.5$  and maximum iteration number 20, where lists are added to until  $L = 4$  or the predicted list-BLER is below  $10^{-5}$ . Upper panel: BLER and BER. Middle panel: average number of queries per-bit until a decoding, where parallelized assumes all rows/columns are decoded in parallel. Lower panel: average number of iterations.

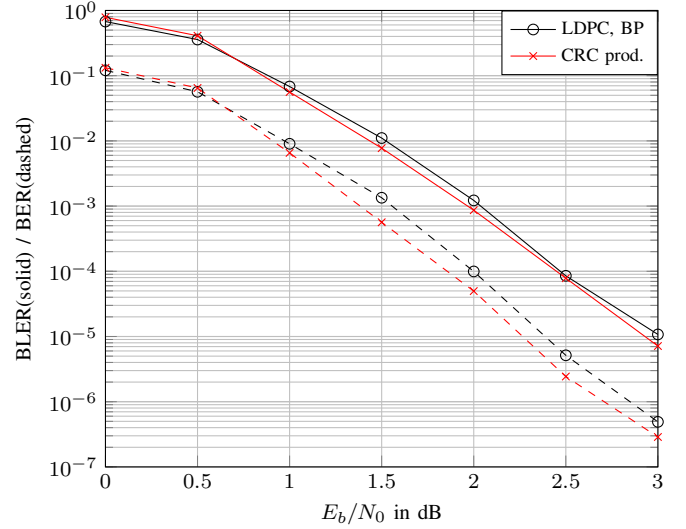


Fig. 6: AWGN performance of the  $(625, 225)$  5G LDPC with max. number of iterations  $I_{\max} = 50$  as compared to a  $(625, 225) = (25, 15)^2$  CRC 2b9 product code decoded using SOGRAND with  $\alpha = 0.5$  and max. iteration 20, where lists are added to until  $L = 4$  or the predicted list-BLER is below  $10^{-5}$ . Upper panel: BLER and BER. Middle panel: average number of queries per-bit until a decoding with SOGRAND, where parallelized assumes all rows/columns are decoded in parallel. Lower panel: average number of iterations.

where  $I_n^{(i)}$  a  $n \times n$  circulant permutation matrix obtained by the right rotation (by 1 position) of the identity matrix. Product codes can be thought of as a special case of the QC-GLDPC ensemble with variable node degree-2.

Block turbo decoding of product codes works as follows (see Fig. 9):

- 0 The channel LLRs are stored in an  $n \times n$  matrix  $\mathbf{L}_{\text{Ch}}$ . The a priori LLRs of the coded bits are initialized to zero, i.e.,  $\mathbf{L}_A = \mathbf{0}$ .
- 1 Each row of  $\mathbf{L}_{\text{Ch}} + \mathbf{L}_A$  is processed by an SISO decoder, and the resulting APP LLRs and extrinsic LLRs are stored in the corresponding rows of  $\mathbf{L}_{\text{APP}}$  and  $\mathbf{L}_E$ , respectively. A hard decision is made based on  $\mathbf{L}_{\text{APP}}$ . If all rows and columns of the decision correspond to valid codewords, the block

turbo decoder returns the hard output, indicating successful decoding. Otherwise,  $\mathbf{L}_A$  is set to  $\alpha \mathbf{L}_E$ , for some  $\alpha > 0$ , and the decoder proceeds to the column update.

- 2 Each column of  $\mathbf{L}_{\text{Ch}} + \mathbf{L}_A$  is decoded and the columns of  $\mathbf{L}_{\text{APP}}$  and  $\mathbf{L}_E$  are updated as step 1. A hard decision is performed using  $\mathbf{L}_{\text{APP}}$ . If the obtained binary matrix is valid, decoding success is declared. If the maximum iteration count is reached, a decoding failure is returned. Otherwise, we set  $\mathbf{L}_A = \alpha \mathbf{L}_E$  and proceed to the next iteration (i.e., return to step 1).

In simulation, we set  $\alpha = 0.5$  and use 1-line ORBGRAND in conjunction with eq. (10) as the SISO SOGRAND decoder. With even codes the demodulated signal is used to identify the parity of the noise effect that is being sought.

Decoding of GLDPC codes is based on the BP principle

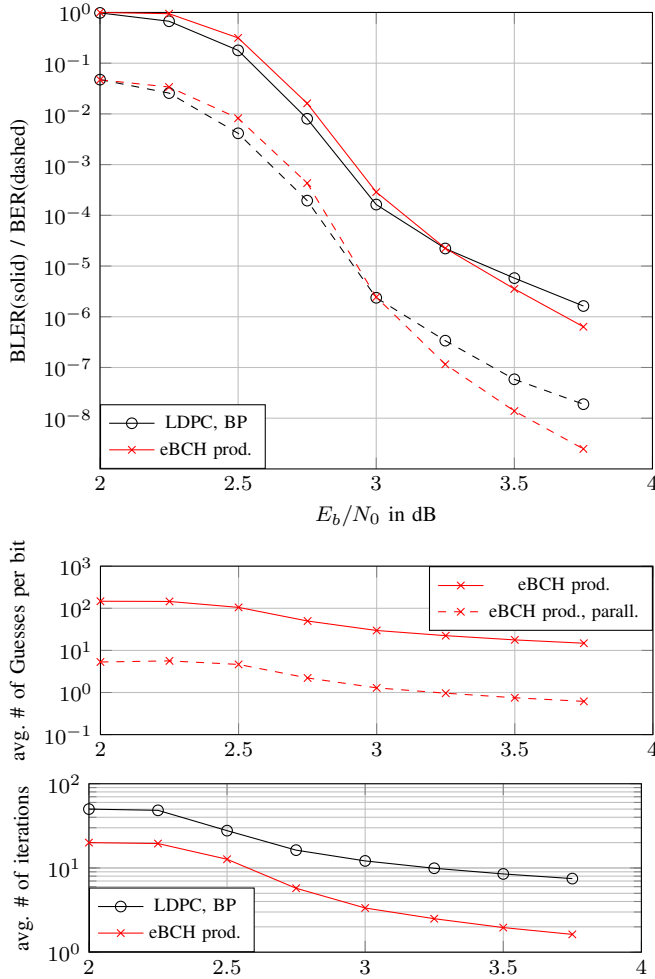


Fig. 7: AWGN performance of the  $(4096, 3249)$  5G LDPC with max. iterations 50 compared to a  $(4096, 3249) = (64, 57)^2$  eBCH product code decoded using SOGRAND with  $\alpha = 0.5$  and max. iteration 20, where lists are added to until  $L = 4$  or the predicted list-BLER is below  $10^{-6}$ . Upper panel: BLER and BER. Middle panel: average number of queries per-bit until a decoding with SOGRAND, where parallelized assumes all rows/columns are decoded in parallel. Lower panel: average number of iterations.

over the Tanner graph which is a generalization of the block turbo decoding of product codes. Each decoding iteration consists of an exchange of soft messages between variable nodes (VNs) and check nodes (CNs). Each CN works as an SISO decoder as described in Sec. V-B, i.e., each CN treats the extrinsic LLRs from last iteration as a-priori information and generates the corresponding extrinsic LLRs. Again, for SOGRAND 1-line ORBGRAND with eq. (10) is used. In simulation, the outgoing extrinsic LLRs are always weighted with the scaling factor  $\alpha = 0.5$ . At the end of each iteration, an APP LLR is calculated for each coded bit, and a hard decision is made. If the resulting binary sequence is a valid codeword, then decoding is declared complete.

To evaluate performance, we consider both AWGN and Rician fading channels. In upper panels, we report BLER and

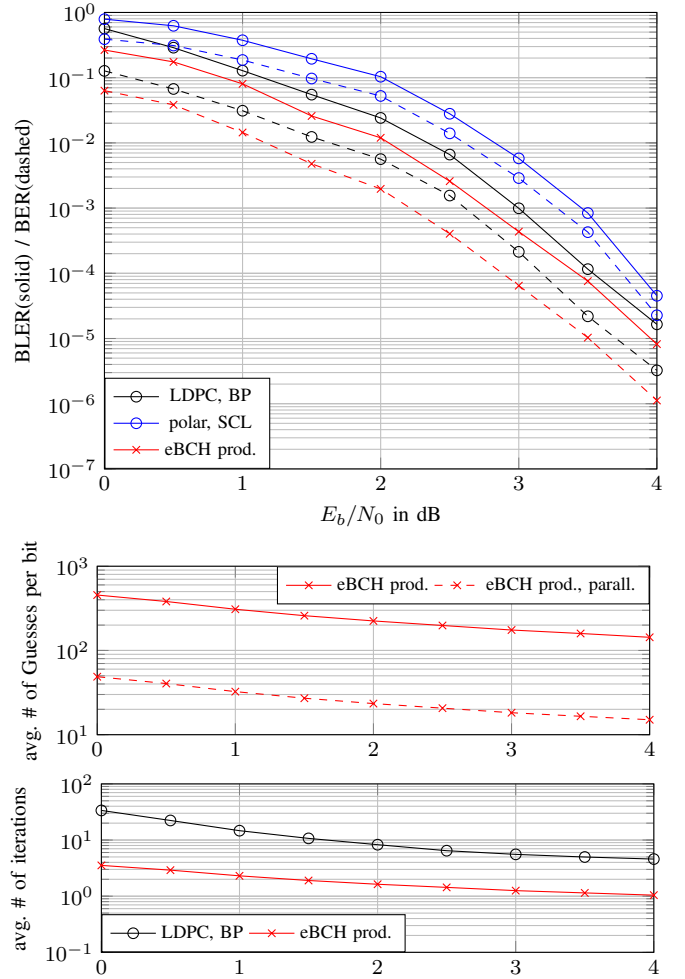


Fig. 8: AWGN performance of the  $(256, 49)$  5G LDPC with max. iterations 50 and the  $(256, 49)$  5G CA-Polar (24-bits CRC) decoded with CA-SCL ( $L = 16$ ) compared to a  $(256, 49) = (16, 7)^2$  eBCH product code decoded using SOGRAND with  $\alpha = 0.5$  and max. iteration 20, where lists are added to until  $L = 4$  or the predicted list-BLER is below  $10^{-5}$ . Upper panel: BLER and BER. Middle panel: average number of queries per-bit until a decoding with SOGRAND, where parallelized assumes all rows/columns are decoded in parallel. Lower panel: average number of iterations.

BER metrics for decoding accuracy. In middle panels, for GRAND-based algorithms we report the average number of queries per coded bit until a decoding has been found and, in the presence of parallelized decoding of rows and columns, the the average sum of the maximum number of queries per-bit, which serve as a proxy for decoding complexity and energy [25, 27, 31], where multiple queries can be made per clock-cycle in hardware. In lower panels, we show the average number of iterations until a decoding is found, which serves as a proxy for latency. In keeping with the existing use for LDPC code decoding, each half-iteration is the largest entirely parallelized unit. For product codes, all rows can be decoded in parallel and all columns can be decoded in parallel.



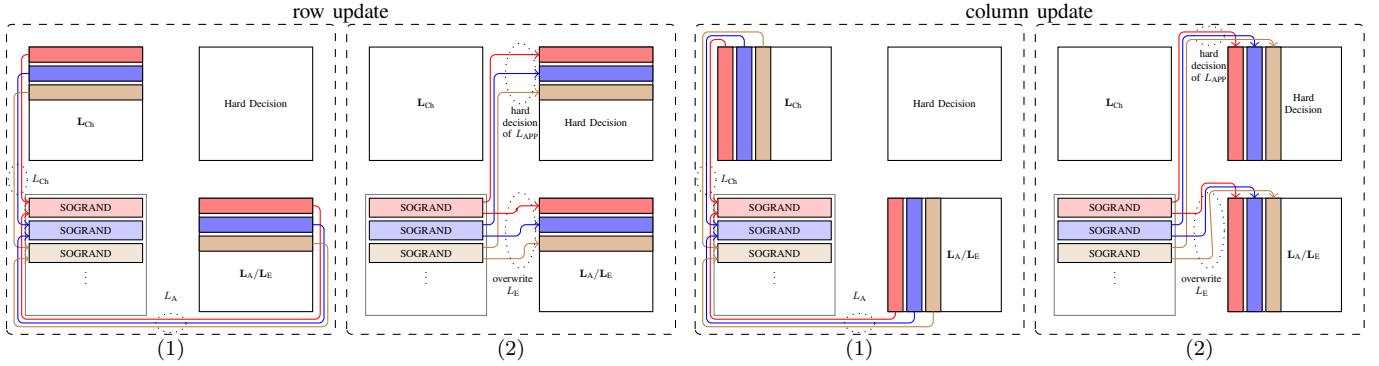


Fig. 9: Block turbo decoding of product codes with SOGRAND.

### A. AWGN Channels

The results in Fig. 1 show that Elias’s original product code can give better BLER performance than a 5G LDPC code when decoded with the new SOGRAND. We first demonstrate that this holds consistently for other code dimensions, where all LDPC codes are from the 5G standard. Fig. 5 shows a comparison for (256, 121) LDPC and a (16, 11)<sup>2</sup> eBCH product code, where it can be seen that the product code outperforms the LDPC in terms of both BLER and BER. The middle plot shows the average number of SOGRAND codebook queries per-bit per product code decoding, showing reduced effort for improved decoding. Note that each iteration of the 1-line ORBGRAND decoding of a product code all rows or column component codes can be decoded entirely in parallel. In that setting, the “parallelized” results in Fig. 5 show the average sum of the maximum number of queries per-bit required for each parallel decoding of all rows or columns, which results in significantly reduced decoding latency. Furthermore, that GRAND codebook queries are themselves parallelizable, which has been exploited in in-silicon realizations where multiple queries are made per clock-cycle [30, 31]. The lower plot demonstrates that the average number of iterations required to identify a decoding is dramatically smaller for the product code than the LDPC code, strongly indicating lower latency decoding.

As GRAND algorithms can decode any moderate redundancy code, the product code construction is not confined to the dRM and eBCH codes reported in Figs 1 and 5. Fig. 6 provides a further example where a (625, 225) LDPC code is compared with a (25, 15)<sup>2</sup> product code that uses a simple cyclic redundancy check (CRC) code as its component code. Again, the product code outperforms the LDPC code with fewer iterations, minimal complexity, and extremely low latency when parallelized. Fig. 7 provides a further comparison for the (4096, 3249) LDPC code and a (64, 57)<sup>2</sup> eBCH product code, resulting in the same conclusion. Fig. 8 provides a further example where a (256, 49) LDPC code is compared with a (16, 7)<sup>2</sup> eBCH product code. Furthermore, the performance of a (256, 49) 5G CA-Polar code with 24-bit CRC decoded with CA-SCL is also provided. As CA-SCL’s complexity increases exponentially with list size, when implemented in hardware, typical list sizes are 2, 4 or 8

[62–64]. Here we allow CA-SCL a generous  $L = 16$  to extract improved performance. Thus, when decoded in an iterative fashion with 1-line ORBGRAND and the new SO as SOGRAND, Elias’s product codes offer comparable or better performance than the LDPC codes selected for 5G new radio (NR). For relatively short and low-rate codes, such as (256, 49), the proposed approach performs slightly better than the CA-Polar code decoded with CA-SCL.

While the LDPC codes used in 5G trade waterfall for an error floor, variants of product codes called GLDPC codes have been developed that have better minimum distance and much lower error floors. As with product codes, GLDPC code components can also be decoded in parallel, which would result in low-latency decoding. Fig. 10 provides results for one such example when a GLDPC developed in [45] is decoded with SOGRAND. The GLDPC results in a significantly steeper waterfall BLER curve with a significantly lower error floor, at the expense of slightly degraded performance at lower SNR, offering more design possibilities for future systems. Again, much fewer iterations are needed for decoding of the GLDPC than the LDPC.

### B. Block Fading Channels

While the results so far have been for AWGN channels, the same conclusions are found for fading channels, as we demonstrate here. Consider a complex-alphabet block fading AWGN channel of coherence block length  $N_c$ . In each coherence block, the transmitted symbols will be affected by the same fading coefficient  $H$ ,  $Y_i = HX_i + Z_i$ ,  $i = 1, \dots, N_c$ , where  $Z_i \sim \mathcal{CN}(0, 2\sigma^2)$ . The noise power spectral density is defined to be  $N_0 = 2\sigma^2$ . If the receiver knows  $H = h$  and, with  $h^*$  being the complex conjugate of  $h$ , computes

$$\frac{1}{h} Y_i = \frac{h^*}{|h|^2} Y_i = X_i + \frac{h^*}{|h|^2} Z_i,$$

then they can form the equivalent channel  $\tilde{Y}_i = X_i + \tilde{Z}_i$ , where  $\tilde{Y}_i = h^* Y_i / |h|^2$  and  $\tilde{Z}_i \sim \mathcal{CN}(0, 2\sigma^2 / |h|^2)$ . Suppose that the channel coefficient  $h$  is estimated as  $\hat{h}$  and Gray labeled

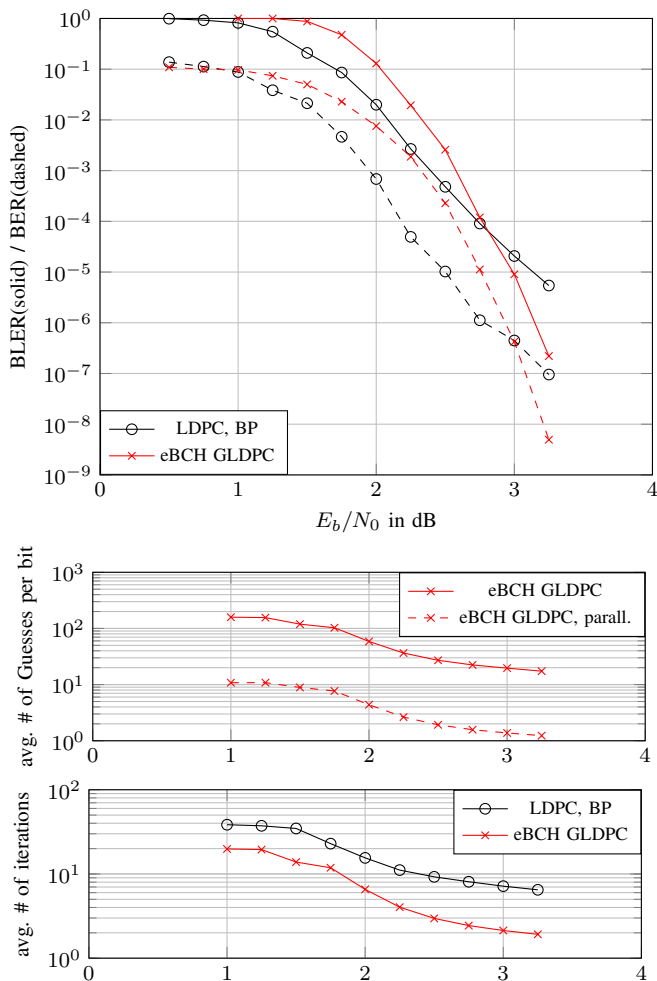


Fig. 10: AWGN performance of the (1024, 640) 5G LDPC with max. iteration 50 as compared to a (1024, 640) GLDPC code [45] with eBCH nodes using SOGRAND with  $\alpha = 0.6$  and max. iteration 20, where lists are added to until  $L = 4$  or the predicted list-BLER is below  $10^{-5}$ . Upper panel: BLER and BER. Middle panel: average number of queries per-bit until a decoding with SOGRAND, where parallelized assumes all rows/columns are decoded in parallel. Lower panel: average number of iterations.

quadrature phase shift keying (QPSK)  $x = f_{\text{QPSK}}(c_1 c_2)$  is used, i.e.,  $\mathcal{X} = \{\pm\Delta \pm \Delta j\}$ . The LLRs of  $c_1, c_2$  are given by

$$\log \frac{p_{Y|C_1, H}(y|0, \hat{h})}{p_{Y|C_1, H}(y|1, \hat{h})} = \frac{2\Delta \Re(y \hat{h}^*)}{\sigma^2}$$

$$\log \frac{p_{Y|C_2, H}(y|0, \hat{h})}{p_{Y|C_2, H}(y|1, \hat{h})} = \frac{2\Delta \Im(y \hat{h}^*)}{\sigma^2}.$$

The SNR is then defined to be

$$\frac{E_s}{N_0} = \frac{\mathbb{E}[\|X\|^2] \mathbb{E}[\|H\|^2]}{2\sigma^2} = \frac{\Delta^2 \mathbb{E}[\|H\|^2]}{\sigma^2}.$$

We consider standard block Rician fading with factor- $K$  [65, 66],  $Y_i = H_{\text{Ri}} X_i + Z_i$ . The fading coefficient of Rician fading is defined by  $H_{\text{Ri}} = \sqrt{K/(K+1)} + \sqrt{1/(K+1)} H_{\text{Ra}}$ , where  $H_{\text{Ra}}$  is the fading coefficient of Rayleigh fading, i.e., the real

part and the imaginary part of  $H_{\text{Ra}}$  are independently Gaussian with zero mean and variance  $\sigma_{\text{Ra}}^2$ , i.e.,  $H_{\text{Ra}} \sim \mathcal{CN}(0, 2\sigma_{\text{Ra}}^2)$ . A high  $K$  factor suggests a more deterministic component in the channel, often due to the predominance of line-of-sight transmission, and as  $K$  becomes very large, the channel approximates an AWGN scenario. Conversely, a low  $K$  factor indicates small-scale fading, usually resulting from a heavily scattered environment, and the channel transitions to Rayleigh fading when  $K$  is zero. Without loss of generality, we set  $\sigma_{\text{Ra}}^2 = 0.5$  such that  $\mathbb{E}[\|H_{\text{Ra}}\|^2] = \mathbb{E}[\|H_{\text{Ri}}\|^2] = 1$ . The codewords are randomly interleaved prior to mapping to QPSK symbols. In each codeword frame of length  $N$  bits, there are  $t$  distinct coherence blocks, i.e.,  $N = 2tN_c$ .

Performance evaluation results are shown in Fig. 11 and Fig. 12 for 1024 bit codes constructed with dRM and eBCH codes, both of which GRAND algorithms can readily decode. Fig. 13 shows equivalent results for a longer 4096 bit code. The results in fading channels mirror those found for AWGN channels, showing that the product codes, when using iterative SOGRAND, significantly outperform Pyndiah's iterative scheme and have better BLER and BER performance compared to 5G LDPCs with BP decoding, in a highly modularized and parallelizable design that has a small number of iterations for decoding.

### C. Encoding Complexity.

Product codes have extremely attractive properties in terms of encoding complexity and latency. To encode each row or column of a systematic code requires only  $k(n-k)$  binary operations, where  $(n-k)$  is small. There are  $k$  such rows and  $n$  columns, resulting in a total complexity of  $(k+n)k(n-k)$ , but all  $k$  components can be encoded in parallel and then all  $n$  components can be encoded in parallel, resulting in a latency of  $2k(n-k)$  which is of order  $k$ . In hardware, for component codes of this size, encoding can be done in one clock cycle so, with full parallelism, encoding would take a total of two clock cycles. The QC structure of the GLDPC codes we present also allows linear complexity encoding as for product codes [67, 68] with similar parallelism for minimal latency.

In contrast, the encoding complexity of LDPC codes can be significant. The naïve application of Gaussian elimination schemes leads to cubic complexity in  $n$ . In order to tackle the complexity issues with LDPC encoding [12], several structures have been imposed on LDPC codes. These constraints include LDPC codes with convolutional codes [69], spatially coupled LDPC codes [70], using the sparsity of LDPC codes for lower triangulation in the encoding matrix [71], restricting the Tanner graphs to exhibit a more product-code-like structure [72], column-scaled LDPC codes [73], dual-diagonal structures [74], increasing field sizes [75, 76], root-protographs structures [77] and, primarily, QC-LDPCs [78]. No such nuance is required with SOGRAND.

## VII. DISCUSSION

Efficient soft-detection decoding of powerful long, low-rate error correction codes has long been a core objective in

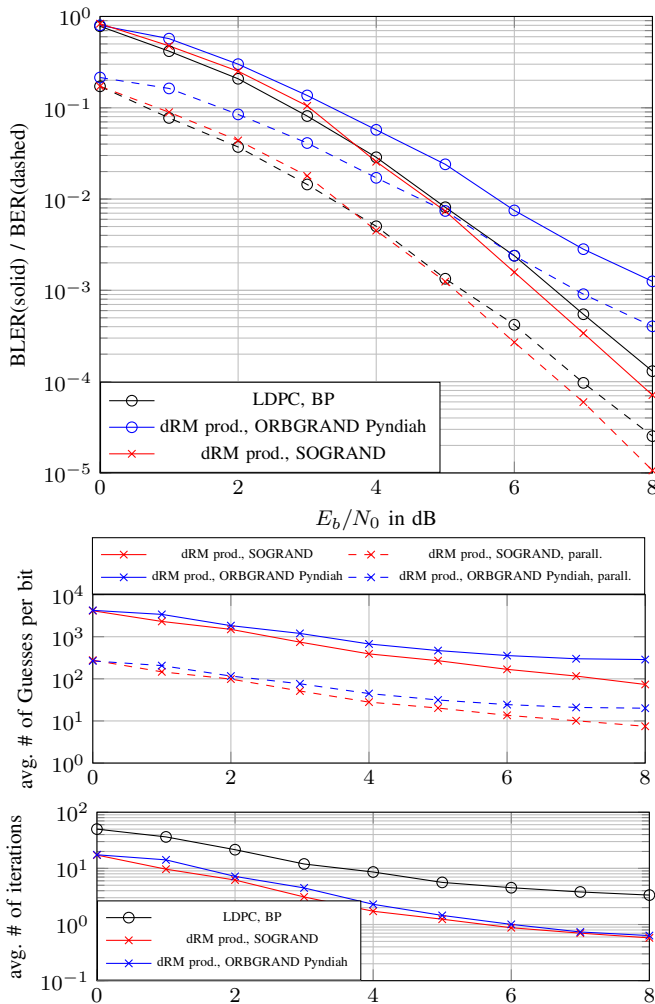


Fig. 11: Block Rician fading channel ( $N_c = 128, t = 4, K = 5$ ) with QPSK decoding performance of the  $(1024, 441)$  5G LDPC with maximum number of iterations  $I_{\max} = 50$  as compared to a  $(1024, 441) = (32, 21)^2$  dRM product code decoded with SOGRAND, i.e. using 1line-ORBGRAND for SO list decoding  $\alpha = 0.5$  and maximum iteration number  $I_{\max} = 20$ , where lists are added to until  $L = 4$  or the predicted list-BLER is below  $10^{-4}$ . Upper panel: BLER and BER performance. Middle panel: average number of queries per-bit until a decoding with SOGRAND, where parallelized assumes all rows/columns are decoded in parallel. Lower panel: average number of iterations.

communications. The successful approach has been to create long codes by appropriate concatenation of component codes that provide SO from their SI in an iterative fashion. Turbo codes use powerful components but approximate SO while LDPC codes use weak components but accurate SO.

Here we demonstrate that GRAND can bridge the gap between Turbo decoding of product codes and LDPC codes by decoding powerful component codes and providing accurate SO with no additional computational burden. We have shown that when decoded with SOGRAND simple product-like codes that avail of powerful, high-rate component codes can outperform the LDPC codes in the 5G standard in fading

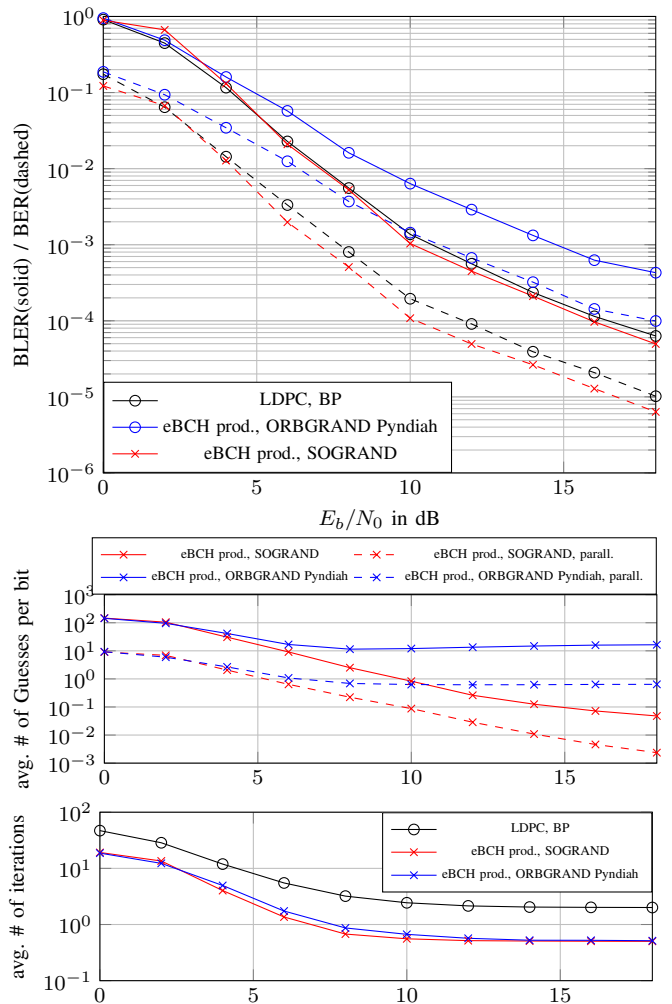


Fig. 12: Block Rician fading channel ( $N_c = 256, t = 2, K = 8$ ) with QPSK decoding performance of the  $(1024, 676)$  5G LDPC with max.iterations 50 compared to a  $(1024, 676) = (32, 26)^2$  eBCH product code decoded with SOGRAND with  $\alpha = 0.5$  and max iterations 20, where lists are added to until  $L = 4$  or the predicted list-BLER is below  $10^{-4}$ . Upper panel: BLER and BER. Middle panel: average number of queries per-bit until a decoding with SOGRAND, where parallelized assumes all rows/columns are decoded in parallel. Lower panel: average number of iterations.

channels. As GRAND algorithms can efficiently decode any moderate redundancy component code, product codes offer a wide design space when decoded with SOGRAND.

Our ultimate goal in this research direction is to design a comprehensive coding scheme that supports all modulation and coding schemes (MCSs) in wireless systems. For example, for high-rate short codes, we directly use GRAND, while for longer codes, we apply SOGRAND with product or GLDPC codes. For higher-order modulations, product codes and GLDPC codes with SOGRAND are fully compatible with BICM, much like LDPC codes. In practical applications, punctured, shortened, or irregular product codes can be employed for rate adaptation and incremental redundancy hybrid automatic repeat request (IR-HARQ). For GLDPC codes, a

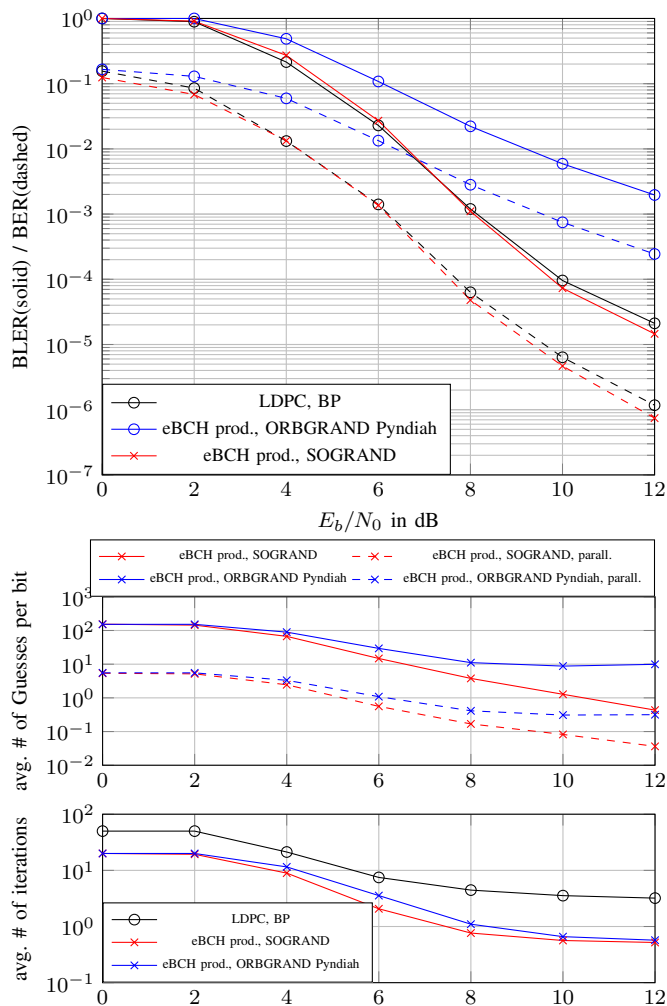


Fig. 13: Block Rician fading channel ( $N_c = 256$ ,  $t = 8$ ,  $K = 6$ ) with QPSK decoding performance of the (4096, 3249) 5G LDPC with max. iterations 50 compared to a (4096, 3249) = (64, 57)<sup>2</sup> eBCH product code decoded with SOGRAND,  $\alpha = 0.5$  and max. iteration number 20, where lists are added to until  $L = 4$  or the predicted list-BLER is below  $10^{-5}$ . Upper panel: BLER and BER. Middle panel: average number of queries per-bit until a decoding with SOGRAND, where parallelized assumes all rows/columns are decoded in parallel. Lower panel: average number of iterations.

Raptor-like structure [79], akin to that used in 5G LDPC codes, could be applied for IR-HARQ.

Circuit designs and a realization of ORBGRAND in hardware [31] illustrate that codebook queries can be parallelised, resulting in low latency, low energy ORBGRAND decoding of component codes. The component codes can be decoded in parallel to generate ultra low-latency long-code implementations. Due to that feature, it is possible to trade-off decoding area versus latency in hardware by determining the number of ORBGRAND circuits in a chip. Moreover, the product-code-like design is highly modular and can be readily adapted to distinct lengths and rates without resorting to puncturing or significantly changing the architecture of the decoder. Product-

like codes also have a significant encoding latency advantage over LDPC codes as all rows and columns (or diagonals) can be encoded in parallel.

While we demonstrate the approach with product and GLDPC codes, a much broad palette of more sophisticated and ultimately more powerful, long, low-rate codes now becomes practical for soft detection decoding, offering a viable alternative to LDPC codes as well as additional possibilities. For example codes such as implicit partial product-LDPC codes [80], which use LDPC codes for rows and BCH codes for columns.

#### ACKNOWLEDGMENTS

The authors would like to thank the Associate Editor and the anonymous reviewers for their valuable comments, which improved the presentation of the work.

#### REFERENCES

- [1] K. Galligan, P. Yuan, M. Médard, and K. R. Duffy, “Upgrade error detection to prediction with GRAND,” in *IEEE Globecom*, 2023.
- [2] C. E. Shannon, “A mathematical theory of communication,” *The Bell System Technical Journal*, vol. 27, no. 3, pp. 379–423, 1948.
- [3] P. Elias, “Error-free Coding,” *Trans. IRE Prof. Group Inf. Theory*, vol. 4, no. 4, pp. 29–37, 1954.
- [4] G. D. Forney, *Concatenated Codes*. MIT Press, 1966.
- [5] C. Berrou, A. Glavieux, and P. Thitimajshima, “Near Shannon limit error-correcting coding and decoding: Turbo-codes,” in *IEEE ICC*, 1993.
- [6] R. Pyndiah, “Near-optimum decoding of product codes: block turbo codes,” *IEEE Trans. Commun.*, vol. 46, no. 8, pp. 1003–1010, 1998.
- [7] R. Gallager, “Low-density parity-check codes,” *IRE Trans. Inf. Theory*, vol. 8, pp. 21–28, 1962.
- [8] D. J. Costello and G. D. Forney, “Channel coding: The road to channel capacity,” *Proc. IEEE*, vol. 95, no. 6, pp. 1150–1177, 2007.
- [9] M. Sipser and D. Spielman, “Expander codes,” *IEEE Trans. Inf. Theory*, vol. 42, no. 6, pp. 1710–1722, 1996.
- [10] D. J. MacKay and R. M. Neal, “Near Shannon limit performance of low density parity check codes,” *Electron. Lett.*, vol. 33, no. 6, pp. 457–458, 1997.
- [11] D. J. MacKay, *Information theory, inference and learning algorithms*. Cambridge university press, 2003.
- [12] T. J. Richardson and R. L. Urbanke, “Efficient encoding of low-density parity-check codes,” *IEEE Trans. Inf. Theory*, vol. 47, no. 2, pp. 638–656, 2001.
- [13] —, “The capacity of low-density parity-check codes under message-passing decoding,” *IEEE Trans. Inf. Theory*, vol. 47, no. 2, pp. 599–618, 2001.
- [14] S.-Y. Chung, G. D. Forney, T. J. Richardson, and R. Urbanke, “On the design of low-density parity-check codes within 0.0045 dB of the Shannon limit,” *IEEE Commun. Lett.*, vol. 5, no. 2, pp. 58–60, 2001.
- [15] M. M. Mansour and N. R. Shanbhag, “High-throughput LDPC decoders,” *IEEE Trans. Very Large Scale Integr. VLSI Syst.*, vol. 11, no. 6, pp. 976–996, 2003.

- [16] D. E. Hocevar, "A reduced complexity decoder architecture via layered decoding of LDPC codes," in *IEEE SiPS*, 2004, pp. 107–112.
- [17] Z. Zhang, V. Anantharam, M. J. Wainwright, and B. Nikolic, "An efficient 10GBASE-T ethernet LDPC decoder design with low error floors," *IEEE J. of Solid-State Circuits*, vol. 45, no. 4, pp. 843–855, 2010.
- [18] P. Hailes, L. Xu, R. G. Maunder, B. M. Al-Hashimi, and L. Hanzo, "A survey of FPGA-based LDPC decoders," *IEEE Commun. Surv. Tutor.*, vol. 18, no. 2, pp. 1098–1122, 2015.
- [19] K.-J. Kim, S. Myung, S.-I. Park, J.-Y. Lee, M. Kan, Y. Shinohara, J.-W. Shin, and J. Kim, "Low-density parity-check codes for ATSC 3.0," *IEEE Trans. Broadcast.*, vol. 62, no. 1, pp. 189–196, 2016.
- [20] T. Richardson and S. Kudekar, "Design of low-density parity check codes for 5G new radio," *IEEE Commun. Mag.*, vol. 56, no. 3, pp. 28–34, 2018.
- [21] K. R. Duffy, J. Li, and M. Médard, "Capacity-achieving guessing random additive noise decoding," *IEEE Trans. Inf. Theory*, vol. 65, no. 7, pp. 4023–4040, 2019.
- [22] K. Galligan, A. Solomon, A. Riaz, M. Médard, R. T. Yazicigil, and K. R. Duffy, "IGRAND: decode any product code," in *IEEE Globecom*, 2021.
- [23] W. An, M. Médard, and K. R. Duffy, "Keep the bursts and ditch the interleavers," *IEEE Trans. Commun.*, vol. 70, no. 6, pp. 3655–3667, 2022.
- [24] K. R. Duffy, M. Médard, and W. An, "Guessing random additive noise decoding with symbol reliability information (SRGRAND)," in *IEEE Trans. Commun.*, vol. 70, no. 1, 2022, pp. 3–18.
- [25] K. R. Duffy, W. An, and M. Médard, "Ordered reliability bits guessing random additive noise decoding," *IEEE Trans. Signal Proc.*, vol. 70, pp. 4528 – 4542, 2022.
- [26] S. M. Abbas, M. Jaleldine, and W. J. Gross, "List-GRAND: A practical way to achieve maximum likelihood decoding," *IEEE Trans. Very Large Scale Integr. Syst.*, no. 1, pp. 43–54, 2022.
- [27] W. An, M. Médard, and K. R. Duffy, "Soft decoding without soft demapping with ORBGRAND," in *IEEE ISIT*, 2023, pp. 1080–1084.
- [28] K. R. Duffy, M. Grundei, and M. Médard, "Using channel correlation to improve decoding – ORBGRAND-AI," in *IEEE Globecom*, 2023.
- [29] A. Cohen, R. G. D'Oliveira, K. R. Duffy, J. Woo, and M. Médard, "AES as error correction: Cryptosystems for reliable communication," *IEEE Commun. Lett.*, vol. 27, no. 8, pp. 1964–1968, 2023.
- [30] A. Riaz, V. Bansal, A. Solomon, W. An, Q. Liu, K. Galligan, K. R. Duffy, M. Médard, and R. T. Yazicigil, "Multi-code multi-rate universal maximum likelihood decoder using GRAND," in *IEEE ESSCIRC*, 2021, pp. 239–246.
- [31] A. Riaz, A. Yasar, F. Ercan, W. An, J. Ngo, K. Galligan, M. Médard, K. R. Duffy, and R. T. Yazicigil, "A sub-0.8pJ/b 16.3Gbps/mm<sup>2</sup> universal soft-detection decoder using ORBGRAND in 40nm CMOS," in *IEEE ISSCC*, 2023.
- [32] L. D. Blanc, V. Herrmann, Y. Ren, C. Müller, A. T. Kristensen, A. Levisse, Y. Shen, and A. Burg, "A GRANDAB decoder with 8.48 Gbps worst-case throughput in 65nm CMOS," in *IEEE ESSERC*, 2024, pp. 685–688.
- [33] C. Condo, V. Bioglio, and I. Land, "High-performance low-complexity error pattern generation for ORB-GRAND decoding," in *IEEE Globecom*, 2021.
- [34] S. M. Abbas, T. Tonnellier, F. Ercan, and W. J. Gross, "High-Throughput VLSI Architecture for GRAND," in *IEEE Workshop on Sig. Proc. Sys.*, 2020, pp. 681–693.
- [35] S. M. Abbas, T. Tonnellier, F. Ercan, M. Jaleldine, and W. J. Gross, "High-Throughput and Energy-Efficient VLSI Architecture for Ordered Reliability Bits GRAND," *IEEE Trans. on VLSI Sys.*, vol. 30, no. 6, 2022.
- [36] C. Condo, "A fixed latency ORBGRAND decoder architecture with LUT-aided error-pattern scheduling," *IEEE Trans. Circuits Sys. I: Regular Papers*, vol. 69, no. 5, pp. 2203–2211, 2022.
- [37] —, "Iterative soft-input soft-output decoding with ordered reliability bits GRAND," in *IEEE Globecom Workshops*, 2022, pp. 510–515.
- [38] K. Galligan, M. Médard, and K. R. Duffy, "Block turbo decoding with ORBGRAND," in *CISS*, 2023.
- [39] R. Hadavian, D. Truhachev, K. El-Sankary, H. Ebrahimzad, and H. Najafi, "Ordered reliability direct error pattern testing (ORDEPT) algorithm," in *IEEE GLOBECOM*, 2023.
- [40] G. Forney, "Exponential error bounds for erasure, list, and decision feedback schemes," *IEEE Trans. Inf. Theory*, vol. 14, no. 2, pp. 206–220, 1968.
- [41] T. Richardson and R. Urbanke, *Modern coding theory*. Cambridge University Press, 2008.
- [42] M. C. Coşkun and H. D. Pfister, "An information-theoretic perspective on successive cancellation list decoding and polar code design," *IEEE Trans. Inf. Theory*, vol. 68, no. 9, pp. 5779–5791, 2022.
- [43] B. P. Smith, A. Farhood, A. Hunt, F. R. Kschischang, and J. Lodge, "Staircase Codes: FEC for 100 Gb/s OTN," *J. Light. Technol.*, vol. 30, no. 1, pp. 110–117, 2012.
- [44] G. Liva, W. E. Ryan, and M. Chiani, "Quasi-cyclic generalized LDPC codes with low error floors," *IEEE Trans. Commun.*, vol. 56, no. 1, pp. 49–57, 2008.
- [45] M. Lentmaier, G. Liva, E. Paolini, and G. Fettweis, "From product codes to structured generalized LDPC codes," in *CHINACOM*, 2010.
- [46] E. Hof, I. Sason, and S. Shamai, "Performance bounds for erasure, list, and decision feedback schemes with linear block codes," *IEEE Trans. Inf. Theory*, vol. 56, no. 8, pp. 3754–3778, 2010.
- [47] 3GPP, "NR; Multiplexing and channel coding," 3rd Generation Partnership Project (3GPP), Technical Specification (TS) 38.21, 2019, version 15.5.0.
- [48] A. Sauter, B. Matuz, and G. Liva, "Error detection strategies for CRC-concatenated polar codes under successive cancellation list decoding," in *CISS*, 2023.
- [49] K. Niu and K. Chen, "CRC-aided decoding of Polar codes," *IEEE Commun. Letters*, vol. 16, no. 10, pp. 1668–1671, 2012.
- [50] I. Tal and A. Vardy, "List Decoding of Polar Codes,"

- IEEE Trans. Inf. Theory*, vol. 61, no. 5, pp. 2213–2226, 2015.
- [51] A. Balatsoukas-Stimming, M. B. Parizi, and A. Burg, “LLR-based successive cancellation list decoding of Polar codes,” *IEEE Trans. Signal Process.*, vol. 63, no. 19, pp. 5165–5179, 2015.
- [52] G. Forney, “The Viterbi algorithm,” *Proc. of the IEEE*, vol. 61, pp. 268–278, 1973.
- [53] A. Raghavan and C. Baum, “A reliability output Viterbi algorithm with applications to hybrid ARQ,” *IEEE Trans. Inf. Theory*, vol. 44, pp. 1214–1216, 1998.
- [54] J. Hagenauer and P. Hoeher, “A Viterbi algorithm with soft-decision outputs and its applications,” in *IEEE Globecom*, vol. 3, 1989, pp. 1680–1686.
- [55] H. Yamamoto and K. Itoh, “Viterbi decoding algorithm for convolutional codes with repeat request,” *IEEE Trans. Inf. Theory*, vol. 26, no. 5, pp. 540–547, 1980.
- [56] S. Lin and D. J. Costello, *Error control coding: fundamentals and applications*. Pearson/Prentice Hall, 2004.
- [57] M. Rowshan and J. Yuan, “Constrained error pattern generation for GRAND,” in *IEEE Int. Symp. on Inf. Theory*, 2022.
- [58] M. Liu, Y. Wei, Z. Chen, and W. Zhang, “Orbgrand is almost capacity-achieving,” *IEEE Trans. Inf. Theory*, vol. 69, no. 5, pp. 2830–2840, 2023.
- [59] E. Arikan, “Channel polarization: A method for constructing capacity-achieving codes for symmetric binary-input memoryless channels,” *IEEE Trans. Inf. Theory*, vol. 55, no. 7, pp. 3051–3073, 2009.
- [60] J. Freudenberger, D. Nicolas Bailon, and M. Safieh, “Reduced complexity hard- and soft-input BCH decoding with applications in concatenated codes,” *IET Circ. Device Syst.*, vol. 15, no. 3, pp. 284–296, 2021.
- [61] T. Hashimoto, “Composite scheme LR+Th for decoding with erasures and its effective equivalence to Forney’s rule,” *IEEE Trans. Inf. Theory*, vol. 45, no. 1, pp. 78–93, 1999.
- [62] X. Liang, J. Yang, C. Zhang, W. Song, and X. You, “Hardware efficient and low-latency CA-SCL decoder based on distributed sorting,” in *IEEE Globecom*, 2016.
- [63] Y. Tao, S.-G. Cho, and Z. Zhang, “A configurable successive-cancellation list polar decoder using split-tree architecture,” *IEEE J. Solid-State Circuits*, vol. 56, no. 2, pp. 612–623, 2021.
- [64] D. Kam, B. Y. Kong, and Y. Lee, “A 1.1 $\mu$ s 1.56Gb/s/mm<sup>2</sup> cost-efficient large-list SCL polar decoder using fully-reusable LLR buffers in 28nm CMOS technology,” in *IEEE Symposium on VLSI Technology and Circuits*, 2022, pp. 204–205.
- [65] R. Steele and L. Hanzo, *Characterisation of Mobile Radio Channels*, 1999, pp. 91–185.
- [66] G. L. Stüber and G. L. Steuber, *Principles of mobile communication*. Springer, 2001, vol. 2.
- [67] Z. Li, L. Chen, L. Zeng, S. Lin, and W. H. Fong, “Efficient encoding of quasi-cyclic low-density parity-check codes,” *IEEE Trans. Commun.*, vol. 54, no. 1, pp. 71–81, 2006.
- [68] T. Zhang and K. Parhi, “A class of efficient-encoding generalized low-density parity-check codes,” in *IEEE ICASSP*, vol. 4, 2001, pp. 2477–2480.
- [69] Z. Chen, S. Bates, D. Elliott, and T. Brandon, “CTH08-5: Efficient encoding and termination of low-density parity-check convolutional codes,” in *IEEE Globecom*, 2006.
- [70] D. G. M. Mitchell, M. Lentmaier, and D. J. Costello, “Spatially coupled LDPC codes constructed from protographs,” *IEEE Trans. Info. Theory*, vol. 61, no. 9, pp. 4866–4889, 2015.
- [71] B. Rajasekar and E. Logashanmugam, “Modified greedy permutation algorithm for low complexity encoding in LDPC codes,” in *ICCICCT*, 2014, pp. 336–339.
- [72] X.-Y. Hu, E. Eleftheriou, and D.-M. Arnold, “Progressive edge-growth Tanner graphs,” in *IEEE Globecom*, vol. 2, 2001, pp. 995–1001.
- [73] S. Zhao, X. Ma, X. Zhang, and B. Bai, “A class of nonbinary LDPC codes with fast encoding and decoding algorithms,” *IEEE Trans. Commun.*, vol. 61, no. 1, pp. 1–6, 2013.
- [74] C.-Y. Lin, C.-C. Wei, and M.-K. Ku, “Efficient encoding for dual-diagonal structured LDPC codes based on parity bit prediction and correction,” in *APCCAS*, 2008, pp. 1648–1651.
- [75] N. B. Chang, “Rate adaptive non-binary LDPC codes with low encoding complexity,” in *ASILOMAR*, 2011, pp. 664–668.
- [76] S. Song, J. Tian, J. Lin, and Z. Wang, “A novel low-complexity joint coding and decoding algorithm for NB-LDPC codes,” in *IEEE ISCAS*, 2019.
- [77] Y. Fang, P. Chen, G. Cai, F. C. Lau, S. C. Liew, and G. Han, “Outage-limit-approaching channel coding for future wireless communications: Root-protograph low-density parity-check codes,” *IEEE Veh. Technol. Mag.*, vol. 14, no. 2, pp. 85–93, 2019.
- [78] I. Djordjevic, S. Sankaranarayanan, and B. Vasic, “Projective-plane iteratively decodable block codes for WDM high-speed long-haul transmission systems,” *J. Light. Technol.*, vol. 22, no. 3, pp. 695–702, 2004.
- [79] T.-Y. Chen, K. Vakili, D. Divsalar, and R. D. Wesel, “Protograph-based raptor-like ldpc codes,” *IEEE Trans. Commun.*, vol. 63, no. 5, pp. 1522–1532, 2015.
- [80] Y. Wang, Q. Wang, and X. Ma, “Design of implicit partial product-LDPC codes and low complexity decoding algorithm,” *IEEE Commun. Lett.*, vol. 27, no. 2, pp. 419–423, 2023.